A ratiometric fluorescent core-shell nanoprobe for sensing and imaging of zinc (II) in living cell and zebrafish

Wandi Chen[1] [na1], Qin Wang[1] [na1], Junping Ma[1,2], Cheuk-Wing Li[2], Mo Yang[3] &

Changqing Yi[1]

Abstract

A zinc(II)-responsive ratiometric fluorescent core-shell nanoprobe (referred to as QPNPs) is described. It consist of an optimized combination of an internal reference dye (TBAP) encapsulated in the core, and a Zn(II)-specific indicator dye (PEIQ) in the shell. The nanoprobe was synthesized via single-step graft copolymerization induced by *tert*-butyl hydroperoxide at 80 °C. QPNPs exhibit a well-defined core-shell nanostructure and well-resolved dual emissions after photoexcitation at 380 nm. After exposure to Zn(II), the QPNPs display a green fluorescence peaking at ~500 nm that increases with the concentration of Zn(II), while the pink fluorescence of the porphine-derived reference dye peaking at ~650 nm remains unchanged. This results in color change from pink to green and thus enables Zn(II) to be detected both spectroscopically and with bare eyes. Zn(II) can be quantified with a 3.1 nM detection limit. The core-shell structured nanoprobe was also applied to real-time imaging of Zn(II) in living HeLa cells and in zebrafish. This work establishes a reliable approach to synthesize ratiometric fluorescent nanoprobes. It enables such nanoprobes to be prepared also by those not skilled in nanomaterial synthesis.

Introduction

Zinc(II) ion is widespread in various human organs such as the brain, retina, intestine, and pancreas, and plays vital roles in many biological processes including neurotransmission, cellular metabolism, protein transcription and regulatory, and etc [1, 2]. Zn(II) is believed to be an essential ionic signal to regulate brain neurotransmitters pass process. Growing evidences suggest that a dysfunction in cellular zinc homeostasis induced by the unbalanced zinc concentration, shows a high risk to cause brain disorder such as epilepsy, cerebral ischemia, and Alzheimer's disease [3]. Hence, in order to study and understand the Zn(II) manner in various organs, the development of rapid and efficient methods for temporally and spatially tracking intracellular zinc ions has become the important subject of current biomedical research.

Fluorometric sensing and imaging with specific probes is an excellent choice for the determination and visualization of the intracellular targets in living cells, owing to its high-speed spatial analysis, and high sensitivity [4,5,6]. Various zinc-specific probes have been designed based on fluorescent nanomaterials, for example, quantum dots [7,8,9,10], carbon nanodots [11, 12], silica nanoparticles [13, 14] and metal nanoclusters [15, 16].

The single-emission fluorescent probes targeting Zn(II) which are operated with a turn-on or turn-off mode, suffer from the easy disturbance by various factors such as probe molecule concentration, environment factors (pH, temperature and polarity), and photobleaching [7,8,9,10,11,12,13,14,15,16]. Therefore, ratiometric probes which use the ratio of two emission intensities to determine the analyte concentration, have been extensively explored for sensitive sensing and imaging intracellular Zn(II) with high accuracy and precision, owing to their built-in correction for environmental effects [17,18,19,20,21]. Most reported ratiometric probes for Zn(II) are based on the mechanisms of internal charge transfer (ICT) and intra-molecular fluorescence resonance energy transfer (FRET). Since the ICT-based ratiometric probes are based on a wavelength shift of a single fluorophore, they always exhibit broad emission spectra with a high degree of overlap before and after binding target ions. This problem of the ICT-based ratiometric probes makes the intracellular imaging of target ions difficult, but can be theoretically avoided by using the FRET mechanism. The FRET-based ratiometric probes are based on the mechanism that the emission of the donor at relative short wavelength induces emission of the acceptor at longer wavelength with their ratio modulated by the target analytes. However, the development of ratiometric Zn(II) probes is still limited by the design and synthesis of either new fluorophores with well-resolved dual emissions or the new energy donor-acceptor pairs.

As a result, it is highly desirable to develop simple and versatile synthetic routes for the preparation of ratiometric probes with enhanced performance in a more efficient way. The use of core-shell structured nanoparticles which consist of an optimized combination of the internal standard encapsulated core and indicator conjugated shell,

appear to be the solution of choice. Therefore, we report the robust preparation of well-defined core-shell structured polymeric nanoprobes, QPNPs, for ratiometric sensing and imaging of Zn(II) in aqueous solution, living cell and zebrafish. In this design, 4,4′,4″,4‴-(porphine-5,10,15,20-tetrayl)tetrakis(benzoic acid) (TBAP) is employed as the internal standard and encapsulated into poly(methyl methacrylate) (PMMA) core, and quinoline derivates PEIQ is employed as zinc-specific indicator and directly presented on the outer polyethylenimine (PEI) shell.

Materials and methods

Materials

Branched PEI, (M.W. 10,000), methyl methacrylate (MMA), *tert*-Butyl hydroperoxide, 8-chloroacetyl-aminoquinoline and TBAP were purchased from Aladdin (http://www.aladdin-e.com/). Penicillin/ streptomycin, fetal bovine serum (FBS), Dulbecco's Modified Eagle Medium (DMEM) high glucose medium, and trypsin were purchased from HyClone (https://www.thermofisher.com/cn/zh/home.html). HeLa cells were obtained from Sun Yat-Sen University Laboratory Animal Center (http://cmc.sysu.edu.cn/main/default/index.aspx).

Synthesis of the QPNPs

First of all, zinc-specific indicator PEIQ was synthesized according to a protocol established in our lab [13]. The detailed synthetic procedures can also be found in the Electronic Supplementary Material. The successful synthesis of PEIQ was confirmed by its ^{1}HNMR spectrum which exhibited the characteristic peaks of both PEI and the intermediate product, 8-(2-chloroacetamido)quinoline (Fig. S1).

QPNPs were synthesized by a one-step emulsifier-free polymerization method [22, 23]. In brief, 0.75 g of PEIQ and 1.5 g of MMA was dissolved in 15 mL of deionized water and the pH value of the mixture was adjusted to 7.0 by HCl solution, followed by the addition of TBAP at different TBAP/MMA (*w*/w) ration (1:200, 1:300, 1:400, 1:500). Then, 250 μL of *tert*-Butyl hydroperoxide (10 mM) was added to induce the graft co-polymerization of TBAP-encapsulated MMA from PEIQ, and the mixture was allowed to react at 80 °C for 2 h under N_2 atmosphere. The resultant QPNPs was collected via centrifugation at 10000 rpm (12,000 g) for 30 min, washed with water and dialysis against D.I water with a tubular membrane of cellulose (MWCO 3.5 kDa). The single-emission fluorescent Zn(II) nanoprobe (referred to as QNPs) which consist of PMMA core without TBAP encapsulation and PEIQ conjugated shell, was synthesized using the similar procedures, only omitting the addition of TBAP.

Instrumentation and characterization

The physiochemical properties of QPNPs, such as the morphology, size distribution, and optical properties, were characterized by JEOL JEM-1400

transmission electron microscopy (TEM), Malvern NanoZS90 instrument, Beckman DU730 UV-Vis spectrometer and Horiba Fluoromax-4P fluorescence spectrometer. The surface functional groups are characterized by an ESCALab250 XPS spectroscopy (Thermo Fisher) using high transmission FAT mode, 14.12 keV, 25 mA, Al Kα (1486.7 eV). Imaging of Zn^{2+} in living HeLa cells and zebrafish with QPNPs was performed using an OLYMPUS IX71fluorescent microscope. z-stack images of cells was taken by a Leica TCS SP5 confocal scanning system.

Sensing Zn(II) in aqueous solution with QPNPs

QPNPs, QNPs, metal ions, and amino acid stock solutions were prepared in water. To evaluate the capability of QPNPs towards aqueous detection of Zn(II), 10 μL of the nanoprobe (1.5 mg mL^{-1}) was firstly mixed with 500 μL of different concentrations of Zn(II) (0, 0.01, 0.03, 0.05, 0.08, 0.10, 0.15, 0.20, 0.30, 0.40, 1.00, 4.00, 8.00 μM) in Tris buffer (100 mM, pH 7.4) for 3 min under gentle shaking. Then, fluorescence images and spectra were captured under 365 nm UV light and photo-excitation at 380 nm, respectively. For comparison, the response of the single-emission fluorescent Zn(II) probe, QNPs (1.5 mg mL^{-1}), was also evaluated using the same procedures.

The practical application of QPNPs for the quantitation of Zn(II) was conducted in the cell extracts [24]. In brief, HeLa cells (1.0×10^6) were collected in the exponential phase of growth. After being washed twice with ice-cold phosphate buffered saline (150 mM, pH 7.4) and re-suspended in ice-cold CHAPS buffer, cell suspension was subjected to the sonication for 30 min followed by centrifugation at 10000 rpm (12,000 g) for 20 min. Then, the suspension was transferred to an EP tube, and used immediately for Zn(II) quantitation by adopting the same sensing parameters and following the same measurement procedures as in aqueous solution.

Imaging of zinc(II) in living HeLa cells and zebrafish with QPNPs

The common human tumor cell, HeLa cells, were cultured at 37 °C under 5% CO_2 with DMEM for imaging intracellular Zn(II). In brief, the living HeLa cells were seeded on 24 well plates (5×10^4 cells per well) and cultured for 24 h to get a suitable density. Then, HeLa cells were incubated with 0.5 mL QPNPs (0.4 mg·mL^{-1}) for 4 h, followed by washed with PBS (150 mM, pH 7.4) three times. After the cells were treated with 20 μM $ZnCl_2$ for 0.5 h, fluorescence images of HeLa cells were captured using an inverted fluorescence microscope, for which the excitation wavelength was set to 380 nm and the emissions were centered at 500 ± 30 nm and 650 ± 30 nm of the double channels.

96 hpf zebra fishes (gifts from Macau University) were employed to perform the in vivo imaging of Zn(II). Healthy zebra fishes were divided into two groups and added into 24 wells plate with 12 larvae per well, followed by being cultured with 2 mL of 0.4 mg·mL^{-1} QPNPs (dissolved in E3 medium) for 4 h. Then, one group was treated with 20 μM Zn(II) for another 0.5 h, the other group without the treatment with Zn(II)

was set as control. Bright filed and FL images were recorded using a fluorescence inversion microscope system (Olympus IX71, Japan).

Results and discussion

Design and sensing rationale of QPNPs

In this study, we intended to develop a new type of ratiometric fluorescent nanoprobe for Zn(II) sensing by sticking to the following design criteria: (1) the ratiometric fluorescent nanoprobe should have well-resolved dual emissions with spectral crosstalk as few as possible; (2) the internal standard and target-specific probes are expected to be excitable at the same wavelength and the same light source; (3) the internal standard and target-specific probes should not undergo FRET [25,26,27,28].

Scheme 1 demonstrates the synthesis route and sensing rationale of QPNPs. In order to meet the above criteria, TBAP and quinoline derivates PEIQ were carefully selected as the internal standard and zinc-specific indicators, respectively. TBAP exhibited strong red emission with a narrow wavelength range of 600–680 nm (curve a of Fig. 1a) and no response towards Zn(II) (curve b of Fig. 1a), authenticating itself an eligible internal standard. PEIQ, a water-soluble zinc-specific indicator, exhibited strong green fluorescence emission with a broad wavelength range of 420–680 nm only in the presence of Zn(II) (curve d of Fig. 1a). It is worthy to mention that PEIQ only exhibited a negligible emission at the wavelength range of 600–680 nm even in the presence of Zn(II) (curve c & d of Fig. 1a), suggesting only limited spectral crosstalk between PEIQ and TBAP. In addition, TBAP and PEIQ can be excited by the same light source and the same wavelength (Fig. 1b).

Scheme 1

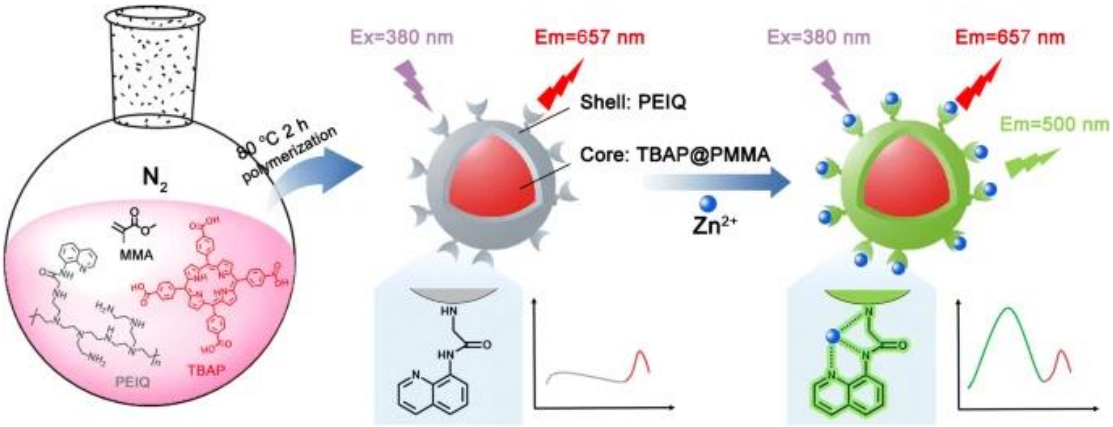

Synthesis route for the core-shell structured nanoprobe QPNPs and its sensing rationale towards Zn(II) through ratiometric fluorescent strategy (PEIQ as the Zn(II) indicator and TBAP as the reference dye)

Fig. 1

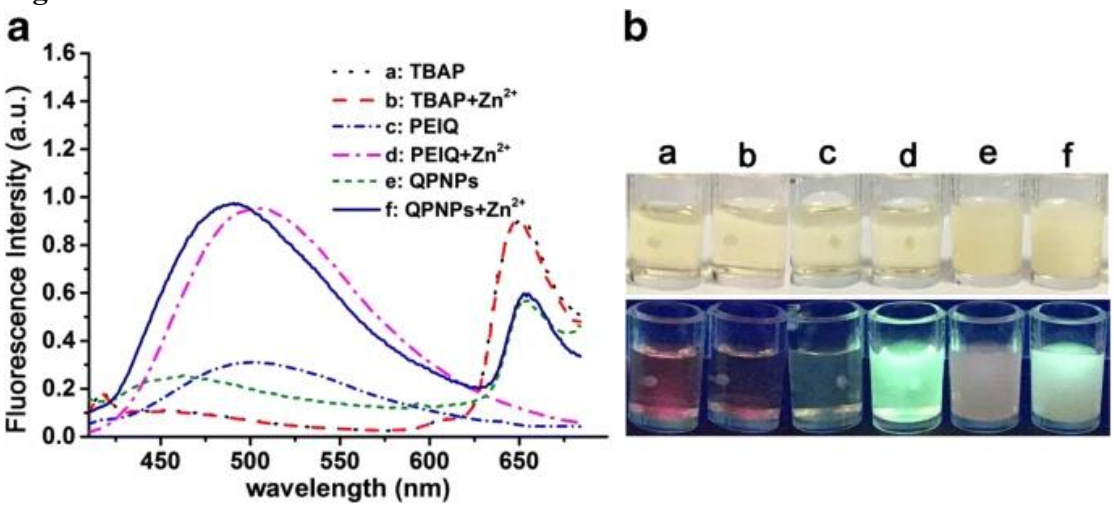

a Fluorescence emission spectrum of TBAP (*a*), TBAP + Zn(II) (*b*), PEIQ (*c*), PEIQ + Zn(II) (*d*), QPNPs (*e*), and QPNPs + Zn(II) (*f*) under photo-excitation at 380 nm; **b** Photographs of aqueous solution containing TBAP (*a*), TBAP + Zn(II) (*b*), PEIQ (*c*), PEIQ + Zn(II) (*d*), QPNPs (*e*), and QPNPs + Zn(II) (*f*), in daylight (upper) and under $\lambda = 365$ nm UV irradiation (lower)

The robust and mild approach for synthesis of the ratiometric fluorescent nanoprobe is essential for sensitive sensing and imaging of targets with high accuracy and precision. In this study, well-defined core-shell structured QPNPs which consist of TBAP-encapsulated PMMA core and quinoline derivates-conjugated PEI shell, are synthesized via a one-step graft copolymerization of TBAP-encapsulated MMA from PEIQ induced by a small amount of *tert*-Butyl hydroperoxide at 80 °C. It is worthy to mention that the diameter of the PMMA core and the thickness of the PEI shell can be finely tuned by controlling the ratio of MMA to PEI [22, 23]. This is quite important because the possible FRET between TBAP and PEIQ can be finely tuned by adjusting the ratio of MMA to PEI. As designed, the QPNPs synthesized using the optimized ratio of MMA to PEI, exhibits a strong fluorescence emission at ~650 nm and a negligible fluorescence emission at ~500 nm in the absence of Zn(II), showing no FRET (curve e of Fig. 1a). After exposure of QPNPs to Zn(II), the fluorescence intensity at ~500 nm induced by the specific and strong coordination between PEIQ and Zn(II) increased obviously. Since the red fluorophore TBAP is not responsive to Zn(II), the fluorescence intensity at ~650 nm remained stable, revealing well-resolved dual emissions without obvious spectral crosstalk and FRET (curve f of Fig. 1a). The specific response of QPNPs towards Zn(II) results in an obvious change of dual emission intensity ratio and a distinct color change from pink to green. This enables the specific and rapid Zn(II) detection by not only spectroscopy but also the bare eyes (Scheme 1 and Fig. 1).

Characterization of QPNPs

Large-area TEM images revealed that both the as-prepared QPNPs and QNPs were spherical in shape with an average diameter of ~160 nm (Fig. S2A & S2C). Dynamic light scattering (DLS) measurements confirmed the uniform size distribution of QPNPs by giving a hydrodynamic diameter of 150 ± 35.0 nm for water-dispersed nanoprobes (Fig. S2B).

The successful preparation of QPNPs which consist of an optimized combination of TBAP-encapsulated PMMA core and PEIQ shell, was validated by the FTIR spectra representing the typical combination of TBAP and PEIQ (Fig. S3A). The presence of surface carboxyl and amine groups on QPNPs was evidenced by the deconvoluted XPS spectra, exhibiting peaks centered at 288.5 eV, 398.8 eV and 531.8 eV which were attributed to C=O, N-H and C-O, respectively (Fig. S3B-S3D).

Properties of QPNPs

The biomedical application of most Zn(II) probes is still severely limited by their weak sensitivity, poor solubility, bad biocompatibility and cell permeability [29]. Benefited from their surface hydrophilic groups including carboxylic and amino groups (Fig. S3), QPNPs are highly water soluble and cell permeable. QPNPs form a homogeneous and transparent yellow aqueous solution without visible precipitation (Fig. 1b). In addition, QPNPs exhibit remarkable long-term colloidal stability in aqueous solution for up to 15 days without forming any aggregation (Fig. S4A).

Polymer matrix can provide an effective barrier to keep the encapsulated dye from the surrounding environment, thus, minimizing its photobleaching phenomena. As expected and demonstrated in Fig. S4B, no obvious photobleaching was observed for QPNPs under continuous irradiation of UV (wavelength = 365 nm) for up to 6 h. In addition, no noticeable amount of TBAP is released into water for up to 14 days (Fig. S4C). The excellent chemo−/photo- stability of QPNPs can facilitate their biomedical applications especially in vivo fluorescence imaging which requires high intensity or prolonged excitations.

Ratiometric sensing of Zn(II) in aqueous solution using QPNPs

The sensing characteristics of QPNPs towards aqueous detection of Zn(II) were optimized at first. Possibly due to the large amounts of PEIQ on the outer surface of an individual QPNPs, the dramatic change in emission color and intensity ratio of the two emission wavelengths (I_{500}/I_{657}) is observed within 2 min. This suggests a rapid response of QPNPs towards Zn(II) (Fig. S5A). Since PEIQ is a pH-insensitive fluorescent Zn(II) probe, a good pH stability of QPNPs is expected. Fig. S5B shows only a negligible influence on the intensity ratio of the two emission wavelengths (I_{500}/I_{657}) in pH range of 4.0–9.0. This enables their use in the physiological pH conditions.

The analytical performance of QPNPs towards aqueous detection of Zn(II) was subsequently evaluated. As shown in Fig. 2a, the green fluorescence intensity centered at ~500 nm continuously increased along with the stepwise addition of Zn(II), whereas the red fluorescence intensity centered at ~657 nm remains constant. The changes in the ratio of two emission intensities cause the fluorescence colors of aqueous solution containing 1.5 mg·mL^{-1} QPNPs changed continuously from pink (no Zn(II)), orange (0.01 μM Zn(II)), yellow (0.03 μM Zn(II)), Kelly (0.05 μM Zn(II)), reseda (0.08 μM Zn(II)) to green (0.10 μM Zn(II)). This enables visual detection of Zn(II) by the bare eye (Inset of Fig. 2a). In order to highlight the advantages of the ratiometric nanoprobe for visual detection, the single-emission fluorescent nanoprobe QNPs was also synthesized and employed for Zn(II) detection. The QNPs consist of PMMA core without TBAP encapsulation and zinc-specific indicator PEIQ conjugated shell. As shown in Fig. 2b, it is quite difficult to use the bare eyes to distinguish the subtle differences among the fluorescence images of aqueous solution of QNPs containing different amount of Zn(II). It is obvious that the dual-emission ratiometric nanoprobe is more sensitive and reliable for visual detection of Zn(II) than the single-emission nanoprobe, although the intensity of the green fluorescence increases at almost the same level.

Fig. 2

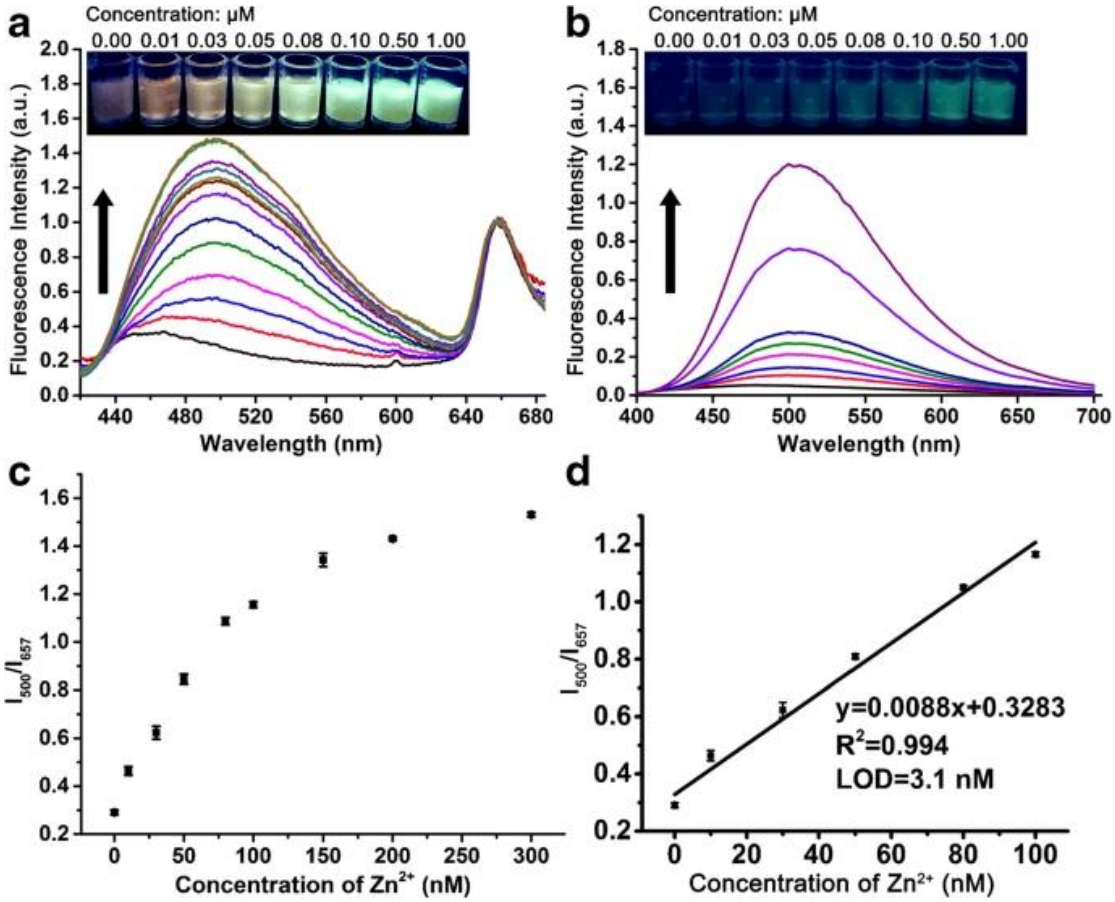

a Ratiometric fluorescent responses of QPNPs upon the exposure to different amounts of Zn(II) under photo-excitation at 380 nm. Inset shows photographs of

QPNPs solutions after exposure to Zn(II) under a 365 nm UV lamp. The concentrations of Zn(II) from left to right are 0, 0.01, 0.03, 0.05, 0.08, 0.10, 0.50, 1.00 μM, respectively. **b** Fluorescence responses of QNPs upon the exposure to different amounts of Zn(II) under photo-excitation at 380 nm. Inset shows photographs of QNPs solutions after exposure to Zn(II) under a 365 nm UV lamp. The concentrations of Zn(II) from left to right are 0, 0.01, 0.03, 0.05, 0.08, 0.10, 0.50, 1.00 μM, respectively. **c** Plot of I_{500}/I_{657} versus Zn(II) concentrations. **d** Linearity of I_{500}/I_{657} against Zn(II) concentrations. Results are mean ± SD of the triplicate experiments

The intensity ratio of the two emission wavelengths (I_{500}/I_{657}) gradually increased with respect to the increasing concentrations of Zn(II) (Fig. 2c), and exhibited a linear range from the 9.1 to 100 nM with a correlation coefficient of 0.994. The limit of detection (LOD) was calculated to be 3.1 nM based on the definition of three times the standard deviation of the blank signal (Fig. 2d). Notably, the dual-emission ratiometric probe QPNPs exhibit a substantially lower LOD and better applicability in the Zn(II) quantitation than most of previously reported nanoprobes [7,8,9,10,11,12,13,14,15,16] (Table S1). Together with its application in absolute aqueous solution without the addition of any organic solvent, QPNPs highlighted its potential applications of Zn(II) quantitation in biological fluids and real-time tracking of Zn(II) in living cells. The concentration of Zn(II) is well documented to range from ~10 μM in plasma to ~0.5 mM in some mammalian cells [30]. Obviously, QPNPs can satisfy the requirements of aqueous quantitation and intracellular imaging of Zn(II).

Because of the complexity of intracellular system, the preparation of fluorescent probes that exhibit high selectivity for target metal ions over other biologically abundant cations is still challenging. Therefore, interference assays were performed by examining the fluorescence response of QPNPs upon the exposure to various metal ions (Al(III), Ba(II), Bi(II), Ca(II), Co(II), Cr(III), Cu(II), Fe(II), Fe(III), Hg(II), K(I), Li(I), Mg(II), Mn(II), Na(I), Ni(II), Pb(II) and Sn(II)) and amino acids (His, Ile, Val, Asp, Thr, Ser, Trp, Pro, Leu, Tyr, Lys, Arg, Ala and Phe). As shown in Fig. 3, most of the coexisting metal ions and all examined amino acids only induced negligible interference to Zn(II) detection, suggesting a decent selectivity for Zn(II) sensing against other biologically abundant cations and amino acids.

Fig. 3

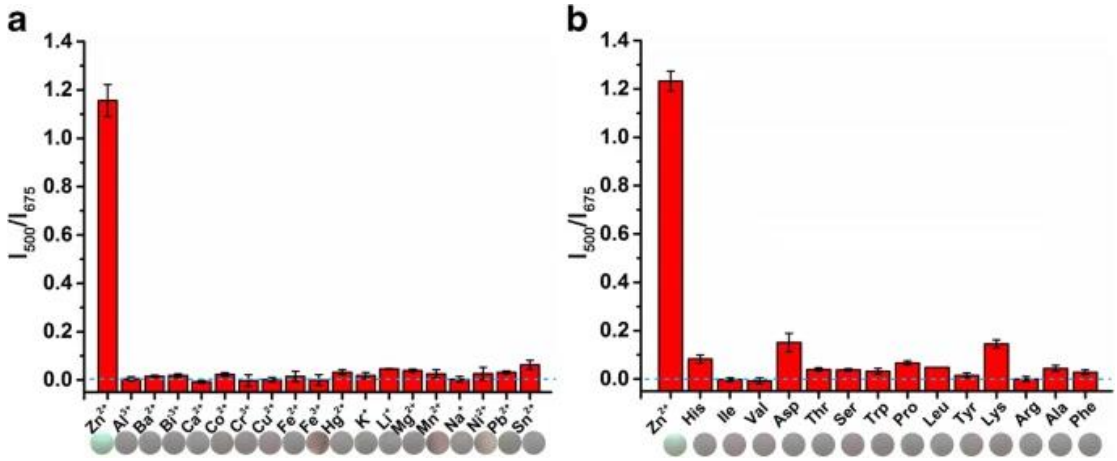

Interference assays. Ratiometric fluorescence responses of QPNPs (1.5 mg·mL^{-1}) towards various metal ions (**a**) and amino acids (**b**). Insets show photographs of QPNPs solutions after exposure to various metal ions and amino acids under a 365 nm UV lamp. Results are mean ± SD of the triplicate experiments

Spiked cell extracts sample analysis using QPNPs

To evaluate the suitability of QPNPs for actual applications in complicated biological environment, Zn(II) spiked in cell extracts was quantified using QPNPs and inductively coupled plasma mass spectrometry (ICP-MS), respectively. For a typical assay, Zn(II) was spiked into the cell extract matrix that has already been determined by ICP-MS to be Zn(II) free, and subsequently subjected to ICP-MS and QPNPs for Zn(II) quantitation. As shown in Table S2 and revealed by the paired Student's t test analysis, there is no systematic difference between the quantitation results using QPNPs and those using the ICP-MS. These results validate the QPNPs as a reliable and practicable nanoprobe for rapid quantitation of Zn(II) in complicated biological environment with decent accuracy and precision.

Intracellular imaging of Zn(II) using QPNPs

Excellent biocompatibility is an essential prerequisite for an ideal bioimaging probe. Therefore, the cytotoxicity of QPNPs towards HeLa cells was evaluated using the classical MTT assays. Results confirmed the outstanding biocompatibility of QPNPs, as evidenced by the impressively high cell viability (>95%) after the treatment with 0.40 mg·mL^{-1} QPNPs for 24 h (Fig. S6A). In addition, the hemolysis assay is also performed to evaluate the hemolytic potential of QPNPs. As shown in Fig. S6B, all the hemolytic efficiency is under 3.0%, indicating the excellent blood compatibility. All these results validate the potential of QPNPs as a low toxic and biocompatible nanoprobe for imaging of Zn(II) in vivo.

Thanks to its abundant surface amino groups which can arouse endosomolytic effect to promote the cell membrane permeability, QPNPs are expected to be capable of crossing cell membrane and thus monitoring intracellular Zn(II) ions [31]. After the

uptake of QPNPs, a strong cellular fluorescence was observed in the perinuclear region of the cytosol (Fig. 4), confirming the good cell-permeability of QPNPs. After the exogenous Zn treatment (20 μM $ZnCl_2$), the cellular fluorescence color turned from red (Fig. 4d) to yellowish green (Fig. 4h). This phenomenon correlates well with the fluorescence spectra and photographs observed in aqueous solution (Fig. 2a), and enables visual identification by the perceived color changes of the probe. And this color change became clearer by observing separated channels. As shown in Fig. 4b and f, the green fluorescence induced by the strong coordination of PEIQ-Zn(II) became brighter after the treatment with Zn(II) source. However, the red reference channel showed almost no change (Fig. 4c and g). Although quantification of intracellular Zn(II) is not yet possible using QPNPs, these results on living cell imaging highlight the potential of core-shell structured polymeric nanoprobe with well-resolved dual-emission for fundamental biomedical research.

Fig. 4

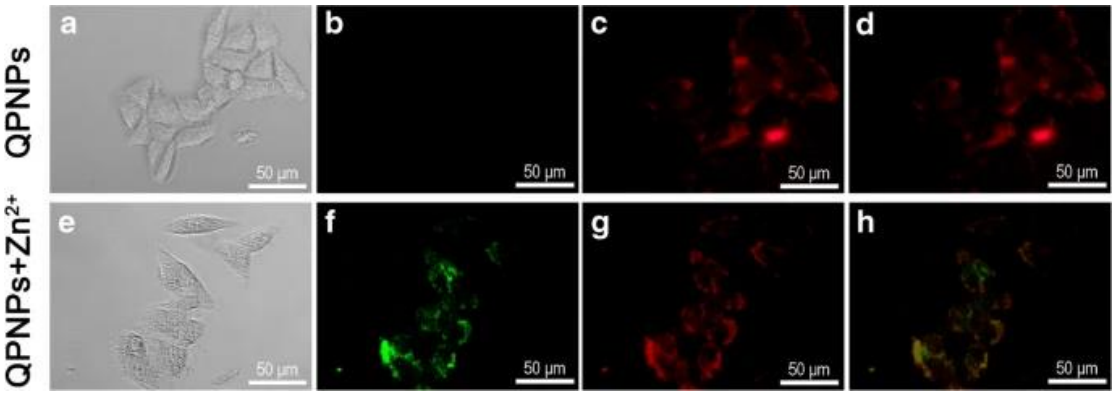

Fluorescence images of HeLa cells incubated with 0.4 $mg \cdot mL^{-1}$ QPNPs for 4 h. **a-d** HeLa cells were treated with QPNPs only. **e-h** HeLa cells were treated with QPNPs followed by treated with 20 μM Zn(II) for another 0.5 h. **a**, **e** the bright-field images; **b**, **f** the fluorescence images obtained from 470 to 530 nm; **c**, **g** the fluorescence images obtained from 570 to 630 nm; **d**, **h** the overlay of the fluorescence images

Full size image

To demonstrate the capability of QPNPs for spatial tracking of intracellular Zn(II), z-stack images of cells from top to bottom at 1-μm "slice" intervals was taken [32]. Fig. S7 is captured in the middle slice of the z-stack, and shows the overlay of the bright-field and fluorescence images of HeLa cells upon incubation with QPNPs in the presence of Zn(II). Specifically, the main section of Fig. S7 shows fluorescence data measured in a plane in the *z* direction, whereas the reconstructed sections of the same cells along *x* and *y* directions are shown at the uppermost and rightmost edge regions of the image, respectively. It is obvious that intimately interconnected three planes (*x*, *y* and *z* direction) which share a common focal center within the cell itself, exhibits evident yellowish green fluorescence simultaneously. Based on these imaging results, it

can be reasonably concluded that QPNPs are internalized within the HeLa cells and can spatially track intracellular Zn(II).

Imaging of Zn(II) in zebrafish using QPNPs

The QPNPs were also employed to trace the distribution of Zn(II) in zebrafish (Fig. 5). It is obvious that QPNPs can be uptaken by the zebrafish, as evidenced by the bright red fluorescence signals observed at the yolk sac (Fig. 5b & g). In the absence of Zn(II), there is no observable green fluorescence in zebrafish (Fig. 5c). After the treatment with Zn(II) (20 μM $ZnCl_2$), the strong coordination of PEIQ-Zn(II) trigger strong green fluorescence emission as observed clearly in separated channels (Fig. 5h). Therefore, the fluorescence color of yolk sac turned from red (Fig. 5d) to yellowish green (Fig. 5i) due to the changes in the ratio of two emission intensities. These results are consistent with the fluorescence spectra and photographs (Fig. 2a) and fluorescence images of the HeLa cells (Fig. 4), validating the feasibility for visual detection of Zn(II) even in vivo. In addition, the bright-field images of the zebrafish confirm their intact morphology upon exposure to QPNPs for more than 4 h, again verifying their excellent biocompatibility (Fig. 5a, e, f & j).

Fig. 5

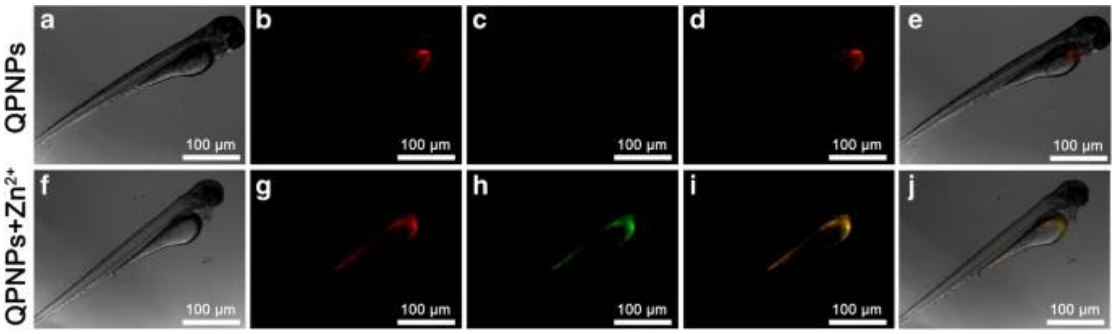

Fluorescence images of 96 hpf zebrafishes incubated with 0.4 $mg \cdot mL^{-1}$ QPNPs for 4 h. **a**-**e** Larvae were treated with QPNPs only. **f**-**j** Larvae were treated with QPNPs followed by treated with 20 μM Zn(II) for another 0.5 h. **a**, **f** The bright-field images; **b**, **g** The fluorescence images obtained from 470 to 530 nm; **c**, **h** The fluorescence images obtained from 570 to 630 nm; **d**, **i**The overlay of the fluorescence images; **e**, **j** The overlay of the fluorescence images and bright-field images

Conclusion

In summary, by preparing core-shell structured and dual-emission QPNPs via a one-step emulsifier-free polymerization, a ratiometric strategy has been successfully developed and demonstrated for rapid and specific biosensing and imaging of Zn(II) in living cells and zebrafish. The QPNPs can quickly recognize Zn(II) with high specificity over other metal ions and amino acids, and the aqueous quantitation of Zn(II) can be achieved with a detection limit of 3.1 nM. Although quantification of

intracellular Zn(II) is not yet possible using QPNPs, Zn(II) imaging in living HeLa cells and zebrafish highlight the potential of QPNPs for fundamental biomedical research. More importantly, this work establishes a reliable and mild approach to design and synthesize the ratiometric fluorescent nanoprobes. Through rationally tailoring the internal standard and outer surface conjugated indicators, it is feasible to use the approach reported in this study to design and prepare fluorescent nanoprobes with well-resolved dual emissions for ratiometric sensing and imaging of other bioactive species in living cells and organisms which are related to pathological and physiological events.

References

1. O'Halloran TV (1993) Transition metals in control of gene expression. Science 261:715–725. https://doi.org/10.1126/science.8342038
2. Berg JM, Shi Y (1996) The galvanization of biology: a growing appreciation for the roles of zinc. Science 271:1081–1085. https://doi.org/10.1126/science.271.5252.1081
3. Frederickson CJ, Koh JY, Bush AI (2005) The neurobiology of zinc in health and disease. Nat Rev Neurosci 6:449–462. https://doi.org/10.1038/nrn1671
4. Giepmans BN, Adams SR, Ellisman MH, Tsien RY (2006) The fluorescent toolbox for assessing protein location and function. Science 312:217–224. https://doi.org/10.1126/science.1124618
5. Que EL, Domaille DW, Chang CJ (2008) Metals in neurobiology: probing their chemistry and biology with molecular imaging. Chem Rev 108:1517–1549. https://doi.org/10.1021/cr078203u
6. Nolan EM, Lippard SJ (2009) Small-molecule fluorescent sensors for investigating zinc metalloneuro-chemistry. Acc Chem Res 42:193–203. https://doi.org/10.1021/ar8001409
7. Luo XB, Wu WB, Deng F, Chen DZ, Luo SL, Au C (2014) Quantum dot-based turn-on fluorescent probe for imaging intracellular zinc(II) and cadmium(II) ions. Microchim Acta 181:1361–1367. https://doi.org/10.1007/s00604-014-1264-z
8. Wu QA, Zhou M, Shi J, Li QJ, Yang MY, Zhang ZX (2017) Synthesis of water-soluble Ag_2S quantum dots with fluorescence in the second near-infrared window for turn-on detection of Zn(II) and Cd(II). Anal Chem 89:6616–6623. https://doi.org/10.1021/acs.analchem.7b00777
9. Ruedas-Rama MJ, Hall EAH (2009) Multiplexed energy transfer mechanisms in a dual-function quantum dot for zinc and manganese. Analyst 134:159–169. https://doi.org/10.1039/b814879a
10. Xu H, Miao R, Fang Z, Zhong XH (2011) Quantum dot-based "turn-on" fluorescent probe for detection of zinc and cadmium ions in aqueous media. Anal Chim Acta 687:82–88. https://doi.org/10.1016/j.aca.2010.12.002
11. Zhang ZM, Shi YP, Pan Y, Cheng X, Zhang LL, Chen JY, Li MJ, Yi CQ (2014) Quinoline derivative-functionalized carbon dots as a fluorescent nanosensor for

sensing and intracellular imaging of Zn^{2+}. J Mater Chem B 2:5020–5027. https://doi.org/10.1039/c4tb00677a

12. Yang MM, Kong WQ, Li H, Liu J, Huang H, Liu Y, Kang ZH (2015) Fluorescent carbon dots for sensitive determination and intracellular imaging of zinc(II) ion. Microchim Acta 182:2443–2450. https://doi.org/10.1007/s00604-015-1592-7
13. Shi YP, Chen ZH, Cheng X, Pan Y, Zhang H, Zhang ZM, Li CW, Yi CQ (2014) A novel dual-emission ratiometric fluorescent nanoprobe for sensing and intracellular imaging of Zn^{2+}. Biosens Bioelectron 61:397–403. https://doi.org/10.1016/j.bios.2014.05.050
14. Rastogi SK, Pal P, Aston DE, Bitterwolf TE, Branen AL (2011) 8-aminoquinoline functionalized silica nancoparticles: a fluorescent nanosensor for detection of divalent zinc in aqueous and in yeast cell suspension. ACS Appl Mater Interfaces 3:1731–1739. https://doi.org/10.1021/am2002394
15. Liu X, Fu CH, Ren XL, Liu HY, Li LL, Meng XW (2015) Fluorescence switching method for cascade detection of salicylaldehyde and zinc(II) ion using protein protected gold nanoclusters. Biosens Bioelectron 74:322–328. https://doi.org/10.1016/j.bios.2015.06.034
16. Hashemi N, Vaezi Z, Sedghi M, Naderi-Manesh H (2018) Hemoglobin-incorporated iron quantum clusters as a novel fluorometric and colorimetric probe for sensing and cellular imaging of Zn(II) and cysteine. Microchim Acta 185:60. https://doi.org/10.1007/s00604-017-2600-x
17. Li W, Fang B, Jin M, Tian Y (2017) Two-photon ratiometric fluorescence probe with enhanced absorption cross section for imaging and biosensing of zinc ions in hippocampal tissue and zebrafish. Anal Chem 89:2553–2560. https://doi.org/10.1021/acs.analchem.6b04781
18. Wu L, Guo QS, Liu YQ, Sun QJ (2015) Fluorescence resonance energy transfer-based ratiometric fluorescent probe for detection of Zn Zn^{2+} using a dual-emission silica-coated quantum dots mixture. Anal Chem 87:5318–5323. https://doi.org/10.1021/acs.analchem.5b00514
19. Han ZX, Zhang XB, Li Z, Gong YJ, Wu XY, Jin Z, He CM, Jian LX, Zhang J, Shen GL (2010) Efficient fluorescence resonance energy transfer-based ratiometric fluorescent cellular imaging probe for Zn^{2+} using a rhodamine spirolactam as a trigger. Anal Chem 82:3108–3113. https://doi.org/10.1021/ac100376a
20. Xu Z, Baek KH, Kim HN, Cui J, Qian X, Spring DR, Shin I, Yoon J (2010) Zn(II)-triggered amide tautomerization produces a highly Zn(II)-selective, cell-permeable, and ratiometric fluorescent sensor. J Am Chem Soc 132:601–610. https://doi.org/10.1021/ja907334j
21. You Y, Lee S, Kim T, Ohkubo K, Chae WS, Fukuzumi S, Jhon GJ, Nam W, Lippard SJ (2011) Phosphorescent sensor for biological mobile zinc. J Am Chem Soc 133:18328–18342. https://doi.org/10.1021/ja207163r
22. Zhu J, Tang A, Law LP, Feng M, Ho KM, Lee DKL, Harris FW, Li P (2005) Amphiphilic core-shell nanoparticles with poly(ethylenimine) shells as

potential gene delivery carriers. Bioconjug Chem 16:139–146. https://doi.org/10.1021/bc049895l
23. Chen J, Zeng F, Wu S, Su J, Zhao J, Tong Z (2009) A facile approach for cupric ion detection in aqueous media using polyethyleneimine/PMMA core-shell fluorescent nanoparticles. Nanotechnology 20:365502–365507. https://doi.org/10.1088/0957-4484/20/36/365502
24. Shi YP, Yi CQ, Zhang Z, Zhang H, Li M, Yang M, Jiang Q (2013) Peptide-bridged assembly of hybrid nanomaterial and its application for caspase-3 detection. ACS Appl Mater Interfaces 5:6494–6501. https://doi.org/10.1021/am401935y
25. Wang XD, Stolwijk JA, Lang T, Sperber M, Meier RJ, Wegener J, Wolfbeis OS (2012) Ultra-small, highly stable, and sensitive dual nanosensors for imaging intracellular oxygen and pH in cytosol. J Am Chem Soc 134:17011–17014. https://doi.org/10.1021/ja308830e
26. Wang XD, Meier RJ, Wolfbeis OS (2012) A fluorophore-doped polymer nanomaterial for referenced imaging of pH and temperature with sub-micrometer resolution. Adv Funct Mater 22:4202–4207. https://doi.org/10.1002/adfm.201200813
27. Xu W, Lu S, Xu M, Jiang Y, Wang Y, Chen X (2016) Simultaneous imaging of intracellular pH and O_2 using functionalized semiconducting polymer dots. J Mater Chem B 4:292–298. https://doi.org/10.1039/c5tb02071a
28. Stich MIJ, Schaeferling M, Wolfbeis OS (2010) Multicolor fluorescent and permeation-selective microbeads enable simultaneous sensing of pH, oxygen, and temperature. Adv Mater 21:2216–2220. https://doi.org/10.1002/adma.200803575
29. Jiang P, Guo Z (2004) Fluorescent detection of zinc in biological systems: recent development on the design of chemosensors and biosensors. Coord Chem Rev 248:205–229. https://doi.org/10.1016/j.cct.2003.10.013
30. Frausto da Silva JRR, Williams RJP (1991) The biological chemistry of the elements: the inorganic chemistry of life. Clarendon Press, Oxford
31. Boussif O, Lezoualc'H F, Zanta M, Mergny M, Scherman D, Demeneix B, Behr JP, Lezoualch F, Lezoualc'H F, Merqny M, Lezoualc'h F, Zanta MA, Mergny MD, Scherman D, Demeneix B, Behr JP (1995) A versatile vector for gene and oligonucleotide transfer into cells in culture and in vivo: polyethylenimine. Proc Natl Acad Sci U S A 92:7297–7301. https://doi.org/10.1073/pnas.92.16.7297
32. Zhou H, Chen J, Sutter E, Feygenson M, Aronson MC, Wong SS (2010) Water-dispersible, multifunctional, magnetic, luminescent silica-encapsulated composite nanotubes. Small 6:412–420. https://doi.org/10.1002/smll.200901276

Acknowledgements

The financial support from Guangdong-HongKong Technology Cooperation Funding Scheme (2016A050503027), Tip-top Scientific and Technical Innovative

Youth Talents of Guangdong special support program (2014TQ01R417), and the Fundamental Research Funds for the Central Universities (Grant No. 17lgjc09) is gratefully acknowledged.